

In Situ and *Ex Situ* Preparations of ZnO/Poly- $\{trans\text{-}[\text{RuCl}_2(\text{vpy})_4]\text{/styrene}\}$ Nanocomposites

Karen Segala,^{*,a,b} Rosilene L. Dutra,^a César V. Franco,^a
Angela S. Pereira^b and Tito Trindade^b

^aDepartamento de Química, Universidade Federal de Santa Catarina,
88040-900 Florianópolis-SC, Brazil

^bDepartamento de Química and CICECO, Universidade de Aveiro, 3810-19 Aveiro, Portugal

As nanopartículas de semicondutores são de grande interesse científico e tecnológico devido ao fato das suas propriedades eletrônicas e ópticas dependerem do tamanho das partículas. Os nanocristais de semicondutores têm sido intensamente investigados, por exemplo, como nanocargas em diversas matrizes poliméricas. Neste trabalho é apresentada a síntese de nanocompósitos obtidos pela incorporação de nanocristais (NCs) de ZnO no copolímero poli- $\{trans\text{-}[\text{RuCl}_2(\text{vpy})_4]\text{/sty}\}$ (sty = estireno e vpy = 4-vinilpiridina). Numa primeira etapa, o copolímero foi preparado por meio da reação entre os monômeros $trans\text{-}[\text{RuCl}_2(\text{vpy})_4]$ e estireno. Em seguida, NCs de ZnO passivados organicamente foram misturados com o copolímero poli- $\{trans\text{-}[\text{RuCl}_2(\text{vpy})_4]\text{/sty}\}$, em CH_2Cl_2 , para produzir filmes poliméricos do nanocompósito após evaporação do solvente (método *ex situ*). As propriedades destes materiais foram comparadas com as de nanocompósitos análogos obtidos a partir da polimerização *in situ* na presença de NCs de ZnO.

Nanosized semiconductor particles are of great scientific and technological interest because of their size-dependent electronic and optical properties. Semiconductor nanocrystals have been investigated, for example, as nano-fillers for diverse polymer matrices in order to produce new optically active materials. Here we report, for the first time, results concerning the preparation of nanocomposites made of ZnO nanocrystals (NCs) incorporated in the co-polymer poly- $\{trans\text{-}[\text{RuCl}_2(\text{vpy})_4]\text{/sty}\}$ (sty = styrene and vpy = 4-vinylpyridine). In a first step, the co-polymer was prepared by reaction of $trans\text{-}[\text{RuCl}_2(\text{vpy})_4]$ with styrene. Then, organically capped ZnO NCs and poly- $\{trans\text{-}[\text{RuCl}_2(\text{vpy})_4]\text{/sty}\}$ were mixed in CH_2Cl_2 to produce cast films of the nanocomposites after evaporation of the solvent (*ex situ* method). The properties of these materials were compared to those of nanocomposites obtained by *in situ* polymerization in the presence of ZnO NCs.

Keywords: ruthenium(II) complexes, nanocomposites, ZnO nanocrystals

Introduction

Semiconductor nanocrystals (NCs) show size-dependent optical properties and have been investigated as new optical materials in the field of nanotechnology.¹ For example, these nanosized particles have been used together with polymers to produce new optically active inorganic/polymer nanocomposites. This approach takes advantage not only of the intrinsic properties of the starting materials but might also result in new properties due to synergistic effects arising from the combination of the inorganic and organic components.² Depending on the nanoparticles'

characteristics and the synthesis/processing of the polymer matrices, there are several synthetic strategies to prepare polymer nanocomposites. Available approaches include sol-gel methods,³ melt-processing^{4,5} and *in situ* polymerization.^{6,7} The homogeneous distribution of inorganic nanoparticles within the polymer matrix and the strong interface adhesion between the matrix and nano-fillers are important aspects to be considered because of their influence in the nanocomposites' performance.⁸ In this context, comparative studies concerning the *in situ* and *ex situ* preparation of new nanocomposite systems are particularly relevant.

Ruthenium complexes have been extensively investigated both from the fundamental and technological points of view. For example, it is well known that Ru

*e-mail: ksegala@uol.com.br; karen@ua.pt; ksegala@feq.unicamp.br

complexes are of great relevance in the fields of catalysis and solar energy conversion.^{9,10} In addition, Ru complexes have been reported to exhibit properties with strong impact on biological systems. Examples include their role as antioxidants¹¹ and their antitumoral activity.¹² However, nanoscale research on the use of Ru complexes as precursors for new composite materials has been scarce. In this work, we report for the first time the preparation of nanocomposites containing ZnO nanocrystals (NCs) dispersed in the co-polymer poly- $\{trans-[RuCl_2(vpy)_4]/sty\}$. This polymer was prepared through reaction of the complex $trans-[RuCl_2(vpy)_4]$ with styrene (sty) using methodologies described previously.¹³ In order to assess the synthetic requirements for the preparation of homogeneous ZnO/poly- $\{trans-[RuCl_2(vpy)_4]/sty\}$ nanocomposites, both *ex situ* and *in situ* techniques have been employed and investigated.

Experimental

All chemicals were supplied by Aldrich, except ethyl acetate (Lab-Scan), trioctylphosphine oxide (topo, 97% purity) and dichloromethane (Fluka). Styrene (Sigma-Aldrich) was treated over a column of neutral aluminium oxide and stored at 4 °C. The polymerization precursors (the “ruthenium blue solution” and the monomer $trans-[RuCl_2(vpy)_4]$, vpy = 4-vinylpyridine) were obtained as described elsewhere.^{14,15} The co-polymer was prepared by reaction of $trans-[RuCl_2(vpy)_4]$ with styrene (sty) using methodologies previously described.¹³ The ZnO NCs were prepared, at room temperature, by dropwise addition of 33.2 mL of an ethanolic solution of tetramethylammonium hydroxide ($N(CH_3)_4OH \cdot 5H_2O$, 0.552 mol L⁻¹) to 100 mL of a dimethylsulfoxide (dmsO) solution 0.101 mol L⁻¹ in $Zn(CH_3COO)_2 \cdot 2H_2O$. The as prepared ZnO NCs were then organically capped with trioctylphosphine oxide (topo).^{16,17} This surface modification step was employed to confer a hydrophobic character to the inorganic NCs, thus promoting their dispersion in the monomers and enhancing their stability in the reaction medium.¹⁸

For the *ex situ* preparation, both components, ZnO/topo NCs and poly- $\{trans-[RuCl_2(vpy)_4]/sty\}$, were mixed in CH_2Cl_2 to produce cast films of the nanocomposite. Firstly, the co-polymer was completely solubilized in 10 mL of CH_2Cl_2 under stirring. The ZnO NCs prepared as described above were then dispersed in an equal amount of CH_2Cl_2 . The blend was prepared by mixing the solutions containing ZnO NCs and co-polymer, under vigorous stirring, until homogenization. The homogeneous mixture was placed in a Teflon mould and the solvent was left to evaporate at room temperature in a well-ventilated fume-cupboard.

The nanocomposites prepared *in situ* were obtained by dispersing the ZnO NCs in the same toluene solution which contained the monomers $trans-[RuCl_2(vpy)_4]$ and styrene. The polymerization was initiated by heating the mixture at 100 °C during 6 h.¹⁹ Both nanocomposites, *in situ* and *ex situ*, were prepared at 1% (m/m) nominal percentage of ZnO NCs in the co-polymer.

The UV-Vis spectra were measured using a Jasco V-560 instrument. Infrared spectra were recorded in the spectral range 250-4000 cm⁻¹, as KBr pellets, using a Mattson 7000 FT instrument. Analyses by transmission electron microscopy (TEM) and energy dispersive X-ray spectroscopy (EDX) were carried out using a Hitachi H-9000-NA microscope operating at 300 kV. For TEM analysis, a small piece of the nanocomposite film was ground, dispersed in 1-butanol and then deposited on a carbon-coated copper grid. Scanning electron microscopy (SEM) was performed using a HR-FESEM Hitachi SU-70 microscope operating at 25 kV. The samples were analysed after being deposited on Al supports and coated with evaporated carbon.

Results and Discussion

Nanocomposites obtained by the simple mixture of poly- $\{trans-[RuCl_2(vpy)_4]/sty\}$ and ZnO NCs were initially prepared to investigate the effects of ZnO NCs on the polymeric matrix. Additionally, nanocomposite samples prepared by the simple blend of the components (*ex situ* method) were also used for comparative purposes with the analogous nanocomposites prepared *in situ*. Both preparation methodologies, *ex situ* and *in situ*, were employed to achieve a nominal load of 1% (m/m) of ZnO/topo in the co-polymer poly- $\{trans-[RuCl_2(vpy)_4]/sty\}$, here used as matrix. Figure 1 shows the absorption (UV-Vis) spectra of the starting ZnO/topo NCs and the derived poly- $\{trans-[RuCl_2(vpy)_4]/sty\}$ -based nanocomposites. The UV-Vis spectrum of the original ZnO colloid (Figure 1, insert), *i.e.*, before any surface modification step, shows an optical feature peaked at 324 nm that is due to nanosized ZnO. This absorption band is assigned to the first electronic transition of the ZnO exciton and is shifted to higher energies when compared to the typical bulk band gap value for ZnO ($E_g = 3.37$ eV or 368 nm at room temperature, r.t.), showing that the average diameter of the ZnO nanoparticles is in the quantum regime.^{18,20} In fact, this has been explained as consequence of quantum size effects occurring in nanosized particles with dimensions comparable to the Bohr radius (a_B) of the exciton of the bulk semiconductor. For the case of ZnO, the enlargement of the band gap due to particle size decrease is expected to occur for diameters comparable (or less) than 4 nm.^{21,22}

After chemical surface modification of the ZnO colloid using the coordinating solvent topo, the resulting sample showed a clear red shift (Figure 1a) of the ZnO excitonic peak in relation to the original colloid (Figure 1, insert). This red shift was attributed to a slight increase of the ZnO NCs average size resulting from the coalescence of the smaller nanoparticles during the surface modification step.²³ This optical feature is still observed in the spectrum of the nanocomposite ZnO/poly- $\{trans\text{-}[\text{RuCl}_2(\text{vpy})_4]\text{/sty}\}$ prepared *in situ* (Figure 1c) but it is not noticeable for the nanocomposite synthesized by the *ex situ* method (Figure 1d). This is probably related to a less dispersion of the ZnO NCs in the polymer for the *ex situ* preparation, hence leading to a decrease in the homogeneous distribution of the ZnO NCs within the polymeric matrix. As will be discussed later, the presence of ZnO NCs within the polymer was further confirmed through EDX mapping of both nanocomposites (*i.e.*, prepared *in situ* and *ex situ*). Finally the most intense band observed at 440 nm (Figure 1) is characteristic of the $trans\text{-}[\text{RuCl}_2(\text{vpy})_4]$ complex, as described in a previous work.¹⁹

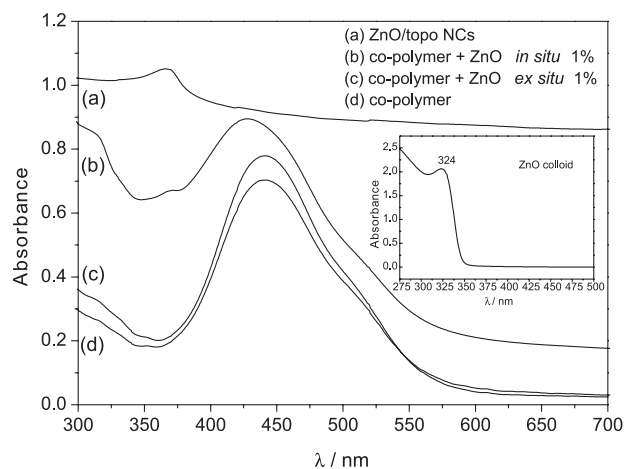


Figure 1. Optical absorption spectra of NCs ZnO/topo (a); *in situ* ZnO/topo NCs nanocomposite (b); *ex situ* ZnO/topo NCs nanocomposite (c) and (d) co-polymer. The insert shows the optical spectrum of the original ZnO colloid.

Figure 2 shows the FTIR spectra of the as prepared ZnO NCs and of ZnO NCs after surface modification with the high boiling point solvent topo. As expected, the FTIR spectrum of the original ZnO NCs (Figure 2a) presents the diagnostic bands at 1576 and 1403 cm^{-1} , related to the symmetrical and asymmetrical stretching modes of the carboxylate groups of acetate coordinated to the surface of the ZnO NCs. Note that the ZnO colloid was synthesized using zinc acetate as the Zn^{II} source. Therefore the ZnO NCs surfaces end up terminated with acetate groups, which confer long-term colloidal stability to the ZnO particles

in dmsO/ethanol.¹⁷ The IR spectrum of the ZnO powder collected after topo treatment of the original ZnO colloid shows a slight shift (1409 and 1577 cm^{-1}) and a decrease in the intensity of the characteristic carboxylate vibrational bands in relation to the diagnostic band of ZnO (441 cm^{-1}). Moreover, there is the appearance of new bands at 2924–2854 and at 1120 cm^{-1} , that are assigned respectively to the stretching vibrational modes of the CH_2 and $\text{P}=\text{O}$ groups of the topo molecules. This is an evidence of partial exchange of acetate groups at the ZnO NCs surfaces by topo molecules and thus accounts for the hydrophobic character of the surface-modified ZnO powders.²⁴

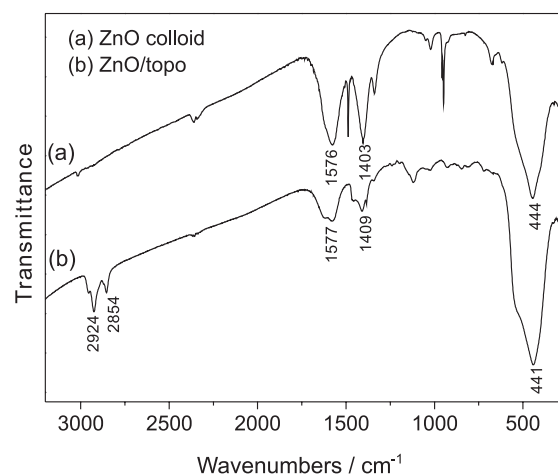


Figure 2. FTIR spectra of powders collected from the original ZnO colloid (a) and after treatment of the ZnO colloid with topo (b).

Figure 3 shows the FTIR spectra for the nanocomposites prepared by the *in situ* and *ex situ* approaches investigated in this work. For the sake of comparison, the FTIR spectrum of the polymeric matrix is also shown. When compared with the spectrum of the polymeric matrix, the FTIR spectra recorded for both *ex situ* and *in situ* nanocomposites show a broad band in the 445–475 cm^{-1} region as a distinctive spectral feature that is due to ZnO NCs dispersed in the polymer.^{18,25} All other vibrational bands are typical of the poly- $\{trans\text{-}[\text{RuCl}_2(\text{vpy})_4]\text{/sty}\}$ used as the matrix.^{14,19} Although the FTIR spectra shown in Figure 3 can only provide a qualitative analysis of the nanocomposites, it clearly reveals that there were no detrimental effects of the ZnO NCs on the polymer, either using the *in situ* or *ex situ* methods for nanocomposite preparation.

The TEM images of the nanocomposite prepared by *in situ* polymerization show ZnO NCs (dark spots) evenly dispersed in the polymer (Figure 4a); conversely, for the *ex situ* prepared nanocomposites, the ZnO NCs are not homogeneously dispersed in the matrix (Figure 4c). However, in both cases the TEM images and size analyses

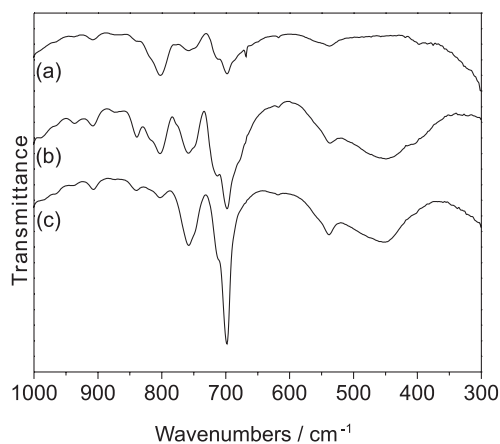


Figure 3. FTIR spectra of KBr pellets containing the co-polymer poly- $\{trans-[RuCl_2(vpy)_4]/sty\}$ (a), the *in situ* prepared nanocomposite (b) and the *ex situ* prepared nanocomposite (c).

show that the ZnO/topo NCs remain morphologically intact after the polymerization process. X-ray powder diffraction confirmed the presence of nanocrystalline ZnO (*wurtzite*) in the polymeric matrix (see insert in Figure 4c for a typical result). The electron diffraction patterns (insert) obtained for these samples appear as diffuse rings (see insert in Figure 4a for a typical result) due to the nanosized dimensions of the crystalline phase, but are still indicative

of ZnO (*wurtzite*). SEM analysis (Figure 5) confirmed a better dispersion of the ZnO NCs within the poly- $\{trans-[RuCl_2(vpy)_4]/sty\}$ for the *in situ* prepared nanocomposites as compared to the *ex situ* counterpart. In fact, the sample obtained by blending poly- $\{trans-[RuCl_2(vpy)_4]/sty\}$ and ZnO NCs appears as a thin film containing large ZnO agglomerates (Figure 5b), while in Figure 5c the ZnO phase appears as more dispersed particulates.

In light of the above discussion, we used EDX mapping to inquire qualitatively the dispersion degree of the ZnO NCs in the polymer, for both the nanocomposites prepared by *ex situ* and *in situ* methods. In the typical SEM images shown in Figure S1 the nanocomposite areas enriched in Zn are labelled in blue while the areas assigned in red are due to the presence of Ru. It is clear that in both nanocomposites the ZnO NCs are well dispersed in the polymeric matrix. However, the *in situ* prepared sample seems more morphologically homogeneous as revealed by a higher density of ZnO NCs (blue regions) throughout the matrix. This result corroborates the discussion above in suggesting that the *in situ* method produces nanocomposites with better homogeneity. There is also a homogeneous distribution of the Ru^{II} complex in the polymeric matrix under analysis, as assigned by the red regions in the EDX mapping.

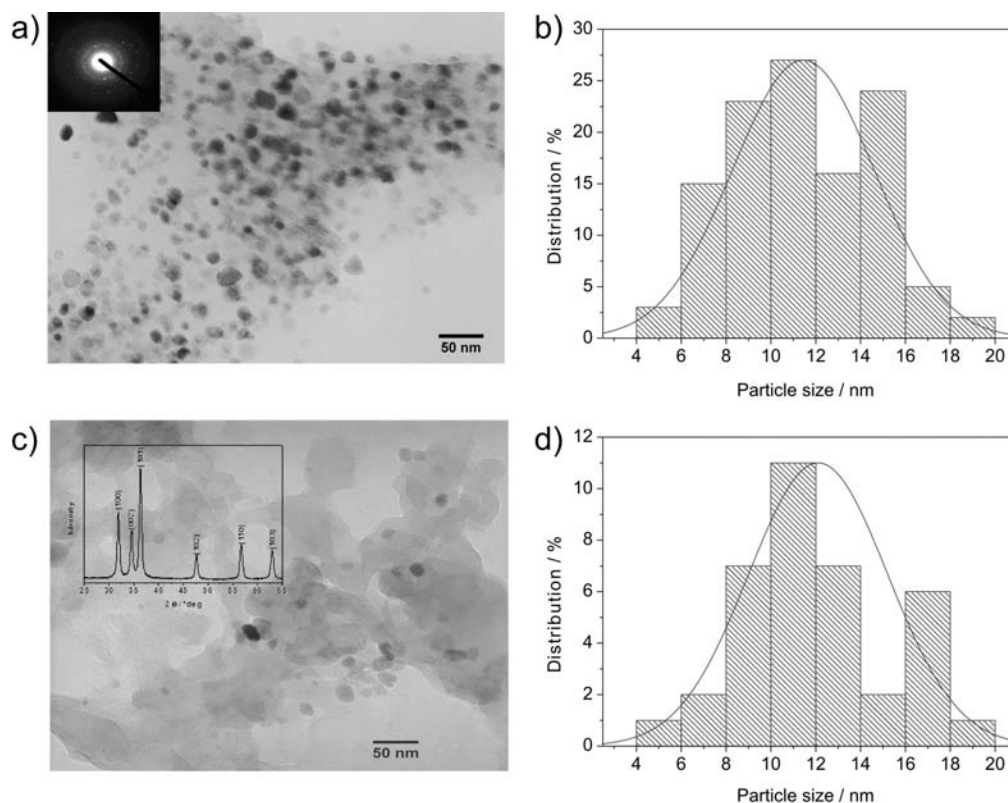


Figure 4. TEM images and histograms obtained for the ZnO/poly- $\{trans-[RuCl_2(vpy)_4]/sty\}$ nanocomposites prepared *in situ* (a and b) and *ex situ* (c and d). The inserts show the corresponding electron and X-ray diffraction patterns of the samples.

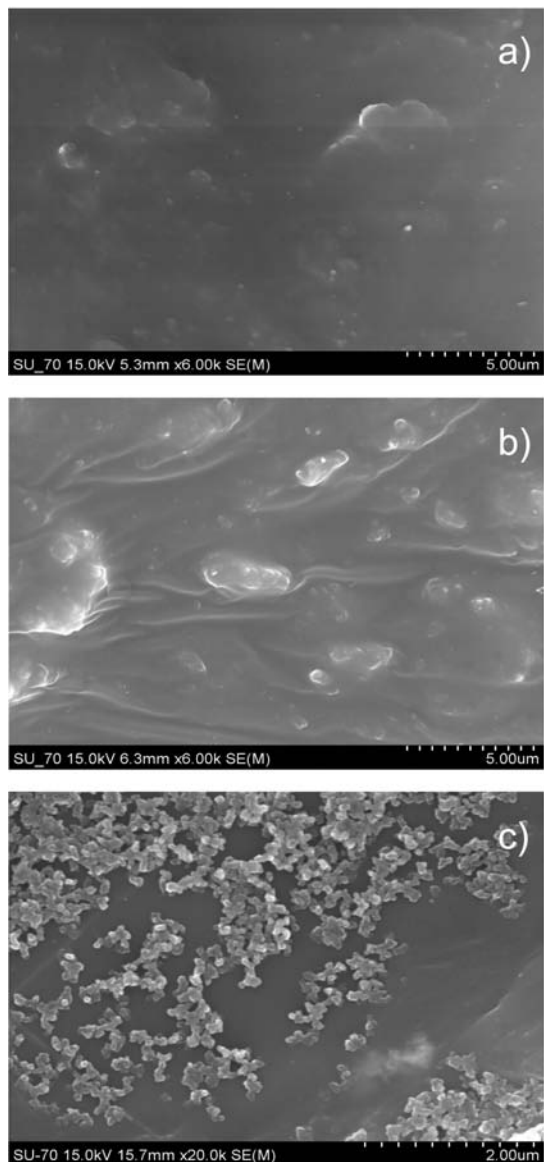


Figure 5. SEM images of poly- $\{trans-[RuCl_2(vpy)_4]/sty\}$ (a), ZnO/co-polymer blend (b) and (c) ZnO/co-polymer obtained by *in situ* polymerization.

In summary, nanocomposites containing ZnO and poly- $\{trans-[RuCl_2(vpy)_4]/sty\}$ have been prepared by *in situ* and *ex situ* strategies and investigated. The results showed that the *in situ* polymerization led to more homogeneous nanocomposites as compared to the blend of the components. This study allows further development of this synthetic strategy to obtain homogeneous nanocomposites of variable composition that can find practical interest in ruthenium-based sensor devices.

Supplementary Information

Supplementary data are available free of charge at <http://jbcs.sbc.org.br>, as PDF file.

Acknowledgments

K. S. thanks CNPq for financially supporting this project and for a research fellowship. The authors would also like to acknowledge the financial support from the Universidade de Aveiro and FCT (Project PTDC/QUI/67712/06).

References

- Trindade, T.; O'Brien, P.; Pickett, N. L.; *Chem. Mater.* **2001**, *13*, 3843.
- Sanchez, C.; Julian, B.; Belleville, P.; Popall, M.; *J. Mater. Chem.* **2005**, *15*, 3559.
- Caruso, R. A.; Antonietti, M.; *Chem. Mater.* **2001**, *13*, 3272.
- Vaia, R. A.; Ishii, H.; Giannelis, E. P.; *Chem. Mater.* **1993**, *5*, 1694.
- Vaia, R. A.; Vasudevan, J.; Krawie, W.; Scanlan, L. G.; Giannelis, E. P.; *Adv. Mater. (Weinheim, Ger.)* **1995**, *7*, 154.
- Huang, X. Y.; Brittain, W. J.; *Macromolecules* **2001**, *34*, 3255.
- Esteves, A. C. C.; Barros-Timmons, A.; Monteiro, T.; Trindade, T.; *J. Nanosci. Nanotechnol.* **2005**, *5*, 766.
- Zhang, F.; Zhang, H.; Su, Z.; *Polym. Bull. (Heidelberg, Ger.)* **2008**, *60*, 251.
- Hagfeldt, A.; Gratzel, M.; *Acc. Chem. Res.* **2000**, *33*, 269.
- Garber, S. B.; Kingsbury, J. S.; Gray, B. L.; Hoveyda, A. H.; *J. Am. Chem. Soc.* **2000**, *122*, 8168.
- Paula, M. M. S.; Pich, C. T.; Petronilho, F.; Drei, L. B.; Rudnicki, M.; Oliveira, M. R.; Moreira, J. C. F.; Henriques, J. A. P.; Franco, C. V.; Dal Pizzol, F.; *Redox Rep.* **2005**, *10*, 139.
- Phillips, A. D.; Gonsalvi, L.; Rornerosa, A.; Vizza, F.; Peruzzini, M.; *Coord. Chem. Rev.* **2004**, *248*, 955; Ravera, M.; Bagni, G.; Mascini, M.; Osella, D.; *Bioinorg. Chem. Appl.* **2007**, 91078.
- Segala, K.; Dutra, R. L.; Oliveira, E. M. N.; Rossi, L. M.; Matos, J. R.; Paula, M. M. S.; Franco, C. V.; *J. Braz. Chem. Soc.* **2006**, *17*, 1679.
- Paula, M. M. S.; Moraes Jr., V. N.; Mocellin, F.; Franco, C. V.; *J. Mater. Chem.* **1998**, *8*, 2049.
- Bandeira, M. C. E.; Prochnow, F. D.; Noda, L. K.; Gonçalves, N. S.; Costa, I.; Melo, H. G.; Crayston, J. A.; Franco, C. V.; *J. Solid State Electrochem.* **2004**, *8*, 244.
- Radovanovic, P. V.; Norberg, N. S.; McNally, K. E.; Gamelin, D. R.; *J. Am. Chem. Soc.* **2002**, *124*, 15192.
- Schwartz, D. A.; Norberg, N. S.; Nguyen, Q. P.; Parker, J. M.; Gamelin, D. R.; *J. Am. Chem. Soc.* **2003**, *125*, 13205.
- Pereira, A. S.; Peres, M.; Soares, M. J.; Alves, E.; Neves, A.; Monteiro, T.; Trindade, T.; *Nanotechnology* **2006**, *17*, 834.
- Franco, C. V.; Paula, M. M. S.; Goulart, G.; De Lima, L. F. C. P.; Noda, L. K.; Gonçalves, N. S.; *Mater. Lett.* **2006**, *60*, 2549.
- Dantas, N. O.; Cardoso, W. A.; Fanyao, Q.; Monte, A. F. G.; Morais, P. C.; Brito Madurro, A. G.; Brito Madurro, J. M.; *Microelectronics J.* **2005**, *36*, 234.

21. Qu, F.; Santos Jr., D. R.; Dantas, N. O.; Monte, A. F. G.; Morais, P. C.; *Physica E* **2004**, *23*, 410.
22. Peres, M.; Costa, L. C.; Neves, A.; Soares, M. J.; Monteiro, T.; Esteves, A. C.; Barros-Timmons, A.; Trindade, T.; Kholkin, A.; Alves, E.; *Nanotechnology* **2005**, *16*, 1969.
23. Cheng, H-M.; Lin, K-F.; Hsu, H-C.; Lin, C-J.; Lin, L-J.; Hsieh, W-F.; *J. Phys. Chem. B* **2005**, *109*, 18385.
24. Kim, C. G.; Sung, K. W.; Chung, T. M.; Jung, D. Y.; Kim, Y.; *Chem. Commun. (Cambridge, U. K.)* **2003**, *16*, 2068.
25. Yang, Y.; Li, Y-Q.; Fu, S-Y.; Xiao, H-M.; *J. Phys. Chem. C* **2008**, *112*, 10553.

Submitted: April 27, 2009

Published online: July 22, 2010